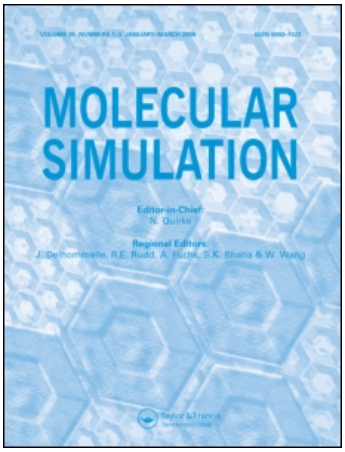

Molecular Simulation
Publication details, including instructions for authors and subscription information:
http://www.informaworld.com/smpp/title~content=t713644482

Structural and dynamic properties of liquid alkali metals: molecular dynamics

F. Juan-Coloa[a]; D. Osorio-González[a]; P. Rosendo-Francisco[a]; J. López-Lemus[a]
[a] Facultad de Ciencias, Universidad Autónoma del Estado de México, Av. Instituto Literario 100, Toluca, México

To cite this Article Juan-Coloa, F. , Osorio-González, D. , Rosendo-Francisco, P. and López-Lemus, J.(2007) 'Structural and dynamic properties of liquid alkali metals: molecular dynamics', Molecular Simulation, 33: 14, 1167 — 1172
To link to this Article: DOI: 10.1080/08927020701586928
URL: http://dx.doi.org/10.1080/08927020701586928

Molecular Simulation, Vol. 33, No. 14, December 2007, 1167–1172

Taylor & Francis
Taylor & Francis Group

Structural and dynamic properties of liquid alkali metals: molecular dynamics

F. JUAN-COLOA, D. OSORIO-GONZÁLEZ, P. ROSENDO-FRANCISCO and J. LÓPEZ-LEMUS*

Facultad de Ciencias, Universidad Autónoma del Estado de México, Av. Instituto Literario 100, CP 50000 Toluca, México

(Received June 2007; in final form July 2007)

Molecular dynamics simulations in the canonical ensemble have been performed to calculate structural and transport properties of liquid alkali metals. The alkali metals considered in this work were Na, K, Rb and Cs. Two Yukawa-type potentials were employed as the interaction law among particles. This function is written in terms of two adjustment parameters which make possible tuning the softness of the potential core and the range of the attractive part. The radial distribution functions and transport properties such as self-diffusion and shear viscosity, were calculated in a thermodynamic state near the melting point. The radial distribution function calculated for each alkali metal was compared with previous simulation results where a more elaborated potential was employed. From this comparison we found an excellent agreement. Our results for transport properties were also compared with the available experimental data and a good agreement was found.

Keywords: Molecular dynamics; Liquid alkali metals; Transport properties; Shear viscosity

PACS: 31.15.Qg

1. Introduction

Traditionally alkali metals have been studied inside an experimental and theoretical framework [1–3]. During the last years with the technology advances and the development of computers, the computer simulation has been of great utility to increase the knowledge about the liquid phase of metals. Frank [4] performed one of first efforts to study the structure of liquid metals.

Physical properties of liquid metals have been studied by means of computer simulation using semi-empirical potentials [5–10]. The embedded-atom method (EAM) proposed initially by Daw and Baskes [11], is one of the most accepted methods to study the physical properties in liquid metals. This semi-empirical potential of n-bodies is based on the density functional theory. This method has been used by Foiles [12] to calculate the static structure factor and the radial distribution function (RDF) for elements such as, Ni, Pd, Cu and Au. Recently, by doing basically Monte Carlo simulations, the EAM has been employed to analyze growth mechanism of Al crystals [13], nanoparticles [14] as well as the liquid–vapor equilibrium for the same metal [15,16]. Another effort for studying metallic fluids, was carried out by Posada-Amarillas and Garzon; they simulate amorphous liquid Ni by molecular dynamics (MD) employing the semi-empirical potential proposed by Gupta [17]. By using both theoretical and MD methods the structure properties for alkali metals were studied [18] considering a local empty-core pseudopotential originally proposed by Hasegawa *et al.* [19]. The structural and dynamic properties for Li have been estimated by means of the orbital-free *ab initio* molecular simulation method [20]. A structural study for Rb and Cs has been done employing *ab initio* molecular simulation method as well [21]. Some theoretical efforts have been performed to estimate the structure factor for rubidium [22]. Balucani *et al.* [7,8], made a study for several alkali metals such as Na, Cs, K and Rb near the melting point using MD, they calculated the RDF for these elements, modeling the molecular interactions with a potential proposed by Price *et al.* [23].

Diverse methodologies have been used for studying the behavior of liquid alkali metals under different thermal conditions. These efforts allow us to observe that the choice of the interaction potential is quite relevant in order to obtain good results. In such a way, the motivation in this

*Corresponding author. Email: jllemus@uaemex.mx

Molecular Simulation
ISSN 0892-7022 print/ISSN 1029-0435 online © 2007 Taylor & Francis
http://www.tandf.co.uk/journals
DOI: 10.1080/08927020701586928

work, is the application of a simple potential to simulate liquid alkali metals. The potential function employed here is basically the Morse function [24] but it is written as two Yukawa-type potentials introducing an extra adjustment parameter. We would like to verify whether this function with just two adjustment parameters is able to reproduce structural and dynamic properties of liquid alkali metals, and then, to estimate the interfacial properties at the liquid–vapor interface for these same kind of fluids. The main objective of this work was to reach the goals of the first point previously mentioned, using a simple potential and a short cut-off radius, mainly because it is desirable to perform molecular simulations investing a short computational time without sacrificing accuracy on data. We performed simulations with MD by using a simple potential in NVT ensemble for some liquid alkali metals. We show the discontinuity that exists in the potential energy near to the melting point. Besides, making use of the Green–Kubo formula [25] both self-diffusion and the shear viscosity are calculated.

This paper is laid out as follows: Section 2 is devoted to describe the interaction potential and some relevant equations are shown. In Section 3, we give a brief but important description of computational details. In the Section 4, the obtained results are shown and compared with available experimental results. And finally, in Section 5 we give the conclusions and the perspectives of this work.

2. Interaction potential and relevant equations

The Morse potential is considered as the interaction law among particles [24,26,27]. This function is written as two Yukawa-type potentials involving an extra adjustment parameter α. This new parameter allows us to modulate the depth of the attractive well. Actually the original Morse function is already written in terms of β which is an adjustment parameter that allows to modify the width of the attractive well.

The original Morse function is written as follows

$$U_M = D\left[e^{-2a(r-r')} - e^{-a(r-r')}\right] \tag{1}$$

where r' is the equilibrium distance where the potential has the minimum well depth $U_M = D$, a being the constant parameter for modulating the width of the attractive well. By doing some identifications $r^* = r/\sigma$ with $\sigma = r' - \ln(2)$ and $\beta = ar' - \ln(2)$ from equation (1) we derive the expression for the reduced Morse function

$$U_M^* = 4\left[e^{-2\beta(r^*-1)} - e^{-\beta(r^*-1)}\right]. \tag{2}$$

The capabilities of this potential have been studied in both homogeneous and inhomogeneous fluids [27,28]. This same function has been widely used for several purposes such as clusters [29] and mechanisms of laser ablation [30]. This potential has also been used to study the size dependence of the melting point in small metallic particles, involving four adjustment parameters [5].

The potential function is written in reduced units as two Yukawa-type potentials

$$U^* = \frac{4}{\alpha r^*}\left[e^{-2\beta(r^*-1)} - e^{-\beta(r^*-1)}\right] \tag{3}$$

where β and α are constant parameters. The factor $1/r^*$ included in equation (3) allows to overcome possible troubles with the thermodynamic stability of the potential, in the sense that the original Morse function remains finite in the origin with a negative contribution which is not associated with any thermodynamically stable state [26,31]. We must mention that we are not interested in the region where the origin is located. Comparing the equation (3) with the original Morse function, the effect of the two adjustment parameters is shown in figure 1.

On the other hand, by means the Green–Kubo formula the transport properties were calculated [25], the self-diffusion is written as follows

$$D = \frac{1}{3}\int_0^\infty \langle v_i(0)\, v_i(t)\rangle \mathrm{d}t, \tag{4}$$

where v_i is the velocity of particle i, and $\langle \ldots \rangle$ denotes the average ensemble. The expression for shear viscosity is

$$\eta = \left(\frac{V}{K_B T}\right)\int_0^\infty \langle P_{ij}(0) P_{ij}(t)\rangle \mathrm{d}t, \tag{5}$$

where K_B is the Boltzmann's constant. V and T represent a given volume and temperature, respectively. P_{ij} are the non-diagonal components of the pressure tensor. The

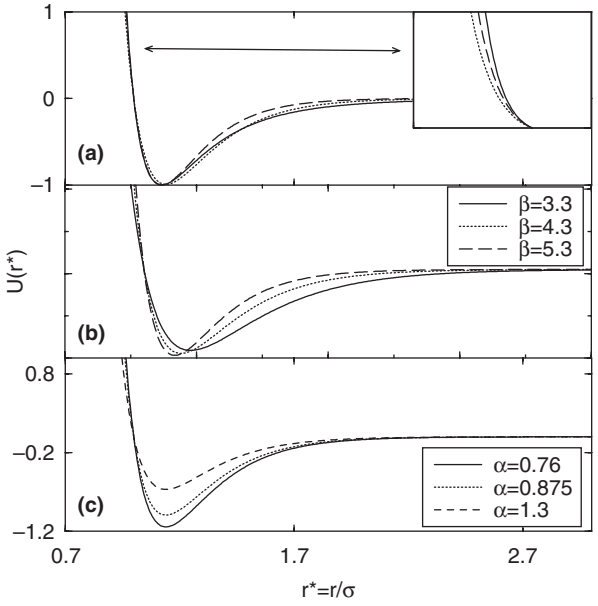

Figure 1. (a) Three potentials are plotted as a function of position, Lennard-Jones (continuous line), original Morse function (dashed line) and two Yukawa-type potentials (dotted line). In the inset we can see the softness of each function. (b) The potential range can be increased when β parameter diminishes by fitting the other parameter. (c) On the other hand, if α parameter increases the intensity of the attraction among particles diminishes, again by fitting the other parameter.

components ($\alpha\beta$) of the pressure tensor are calculated through the virial expression

$$P_{\alpha\beta}V = \sum_{i=1}^{N} m_i v_{ia} v_{i\beta} + \sum_{i=1}^{N-1} \sum_{j>1}^{N} (r_{ij})_a (f_{ij})_\beta, \qquad (6)$$

where r_i and m_i are the position and mass of particle i, respectively. From this identification $r_{ij} = r_i - r_j$. Finally, f_{ij} is the force between two particles i and j.

3. Simulation details

In all our NVT simulations we have used a fcc array placed in a cubic cell as the initial configuration. The leap-frog algorithm was used to move particles implementing periodic boundary conditions and minimum image convention in the three directions. The temperature was maintained constant by means of the Nose–Hoover thermostat with $v_T = 5$ [32, 33]. We have used a cut-off distance of $R_c = 2.5_\sigma$. The neighbor list was also implemented in order to speed up the code [25].

Reduced potential energy was calculated around the melting point. The characteristic parameters for each one of the alkali metals considered in this work as well as the values of reduced density and temperature that were used here, are contained in table 1. For these same thermodynamic states the radial distribution function has been estimated using a particle number of $N = 500$. The reduced time step was $\Delta t = 0.005\sigma(m\epsilon)^{1/2}$. In order to reach the equilibrium 2.5×10^5 steps were performed. The average values were evaluated for additional 2.5×10^6 steps.

On the other hand, the transport properties such as self-diffusion, $D^* = D\sqrt{(m/\epsilon)}/\sigma$, and shear viscosity, $\eta^* = \eta\sigma^2/\sqrt{m\epsilon}$ have been calculated by means of the Green–Kubo formula. To estimate these properties we employed two different particle number $N = 500$ and 2000, in a thermodynamic state that corresponds to liquid phase near the melting point (table 1). The dynamic properties were calculated at the end of simulation storing the particle velocities and non-diagonal pressure components, each 10 time step and each 1 time step, respectively. For self-diffusion the number of particle velocities stored was $N_{\text{vel}} = 256$ in all cases. The reduced time step was $\Delta t = 0.0025$. To obtain numerical values for transport properties both the time dependent diffusion and time dependent shear viscosity were evaluated at $t^* = 1.515$ and 1.5012, respectively. These results are contained in table 2. About 5×10^6 integration steps were performed in order to reach the equilibrium and to obtain averages 2×10^6 extra cycles were carried out. At the same time, the normalized velocity autocorrelation function (VACF) and the stress autocorrelation function (SACF) were calculated.

Table 1. Characteristic parameters for each considered alkali metallic fluid.

Element	*T(K)*	$\rho(\text{Å}^{-3})$	$\epsilon/K_B(K)$	σÅ	α	β
Na	376	0.01045	445.60	3.328	0.31	1.85
Rb	318	0.01284	402.20	4.408	0.32	1.81
K	343	0.02429	420.99	4.115	0.315	1.83
Cs	308	0.00830	386.49	4.761	0.32	1.83

Table 2. Transport properties calculated by MD. Self diffusion and shear viscosity data are written in units $10^{-5}(\text{cm}^2/\text{s})$ and (mp), respectively. Experimental results were taken from Balucani *et al.* [8].

Element	D_{MD}	D_{Exp}	η_{MD}	η_{Exp}
Na	3.91	4.06–4.35	6.46	6.68
Rb	2.63	2.60	6.58	5.52– 6.44
K	3.66	3.52–3.72	5.22	5.14–5.25
Cs	2.17	2.16	6.30	6.50

4. Results and discussion

The potential used in this work is compared with Lennard-Jones and Morse potentials. The softness associated to each potential as well as the reach of the attractive part are shown in the figure 1a. From this comparison it is observed that the potential used here is softer and at the same time has a longer range than the original Morse function. In figure 1b, it is shown that the reach of the attractive well is tuned by the parameter β. Every time we reduce this parameter the width of the attractive part increases. On the other hand, in figure 1c, we can see that the intensity of the attractive interaction can be modulated with the parameter α, in fact, the depth of the attractive well can be reduced when this parameter takes large values. The fitted parameters for each alkali metal are contained in table 1. In figure 2a, it is shown the radial distribution function of Cs estimated by using Morse and modified Morse functions. Both data were compared with results obtained by Balucani *et al.* [8]. Clearly the RDF computed with original Morse function shows differences in comparison to the others curves. In contrast, the RDF obtained with modified Morse potential, agrees very well with the result reported in Ref. [8]. As a matter of fact, they are indistinguishable on the scale of the figure. Figure 2b, shows the RDF calculated for each alkali metal considered in this work and compared against those reported in Ref. [8], and as we can notice the agreement is excellent.

In figure 3, the caloric curve of the considered alkali metals is shown. The potential energy is plotted versus temperature, the discontinuity on the energy evidences the localization of the melting point. The wideness on this discontinuity is the latent heat of fusion. The obtained results were 2.41, 2.24, 2.03 and 2.16 kJ/mol for Na, K, Cs and Rb, respectively. Comparing with the data taken from Chem-Globe database [34], we can notice that the largest difference is around 7% and it corresponds to Na. These results let us mention that the chosen parameters α and β for each simulated alkali metal are correct.

In figure 4, the normalized velocity autocorrelation function is plotted for two temperatures. The upper curve

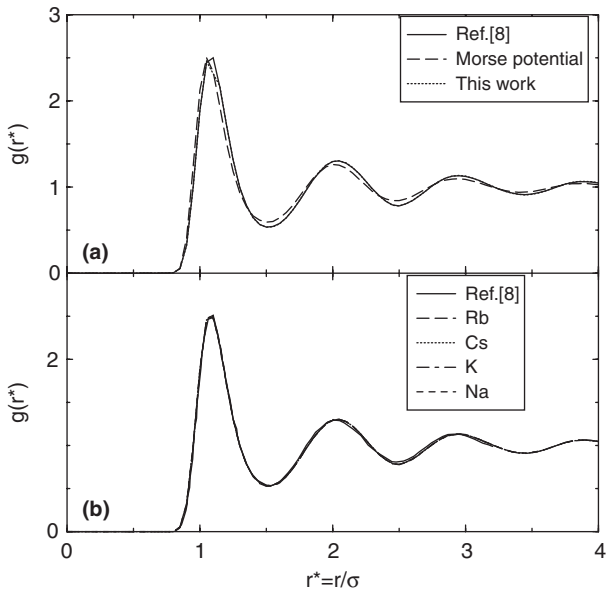

Figure 2. (a) Radial distribution function for Cs. The dashed and dotted lines were generated using Morse and two Yukawa-type potentials, respectively. There are not differences between our results and that from Ref. [8] (continuous line). (b) The RDF is shown for each alkali metal computed by MD. The continuous line corresponds to Ref. [8] for Rb, K and Cs. Our results are shown by means of discontinuous lines: long-dashed (Rb), dotted (Cs), dot-dashed (K) and dashed (Na). No significant differences were found among these curves.

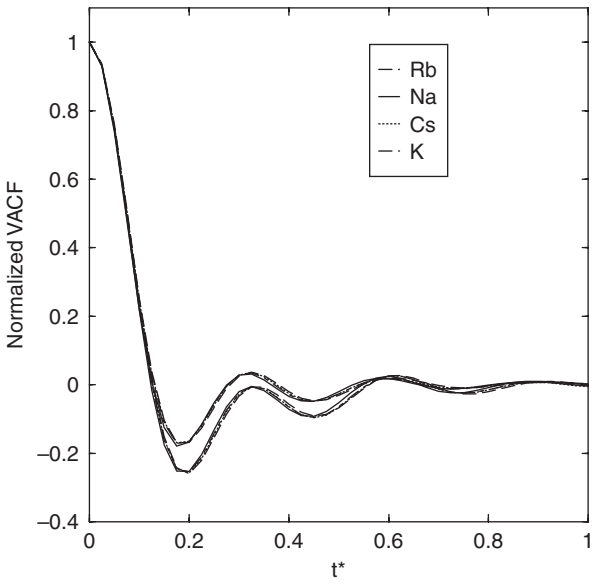

Figure 4. The normalized VACF against the reduced time for two temperatures, $T = 438$ K upper and $T = 500$ K lower. Continue line (Na), dashed line (Rb), dotted line (Cs) and dot-dashed line (K).

corresponds to the normalized VACF function estimated at $T = 438$ K and the lower curve at $T = 500$ K. The negative minimum for short times, that denotes the *cage effect* [35] for fluids with high density, can be observed with the potential used here. This effect takes place when particles collide with their neighbors and their movement changes from the original direction. As a result a particle is caught in a cage which is set by neighboring particles and only after a certain time it is able to escape from such cage. In figure 5, the normalized stress autocorrelation functions, SACF, is shown for these same fluids. In this same figure there is a comparison with the results obtained by Balucani *et al.* [8]. And as a result we can see that the obtained agreement is good. The numerical values to transport properties have been collected in table 2. The self-diffusion was estimated using two different particle number $N = 500$ (not shown) and $N = 2000$, and in fact, using this last option we obtained our best results,

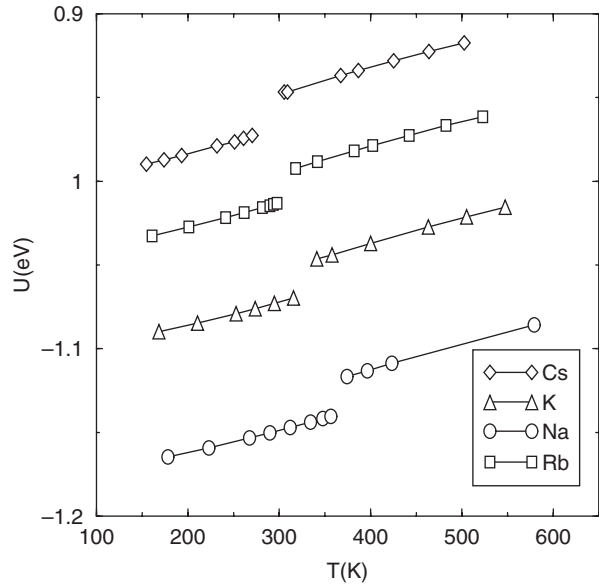

Figure 3. Caloric curve for alkali metals. The discontinuity indicates the localization of the melting point, and the width corresponds to latent heat of fusion. The continuous line is included in order to guide the eye.

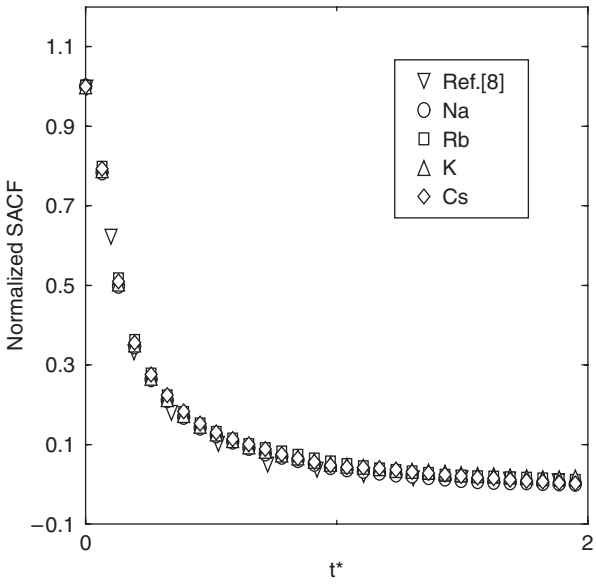

Figure 5. The normalized SACF versus reduced time. Our results are represented through different symbols: circles (Na), squares (Rb), triangles pointing up (K) and diamonds for (Cs). The open pointing dawn triangles correspond to data taken from Ref. [8].

the largest difference is around 3.7% and corresponds to Sodium, our result is shorter than experimental one reported in Ref. [8]. It is well known that the diffusion is a quantity which depends in an important way on particle number when it is obtained by means of the MD [27,36], whereas the shear viscosity does not show such dependence on particle number, that is why it is not important the election of N to estimate this dynamic property. The shear viscosity calculated here for these metals is in agreement with experimental data. The largest difference is around 3% for Sodium, in this case our result is overestimated when comparing with those experimental data which were taken from Ref. [8]. An extra MD simulation was carried out by using the original Morse function with an adjustment parameter (equation (2)) to estimate the transport properties for Cs and compared with our results. The calculated shear viscosity (6.03 mp) is around 4% lower than our results, this means that, the Morse results are 7% lower than the experimental data [8]. For self diffusion (2.9×10^{-5}cm^2/s) we obtained a difference around 25.52% respect to the experimental data and 25.17% respect to our results. Comparing these last two results, we can see a difference around 0.4%.

The relevance of the tail in the oscillating potential proposed by Price *et al.* [23], has already been discussed [22]. And as it is well known, the shape of the potential is quite relevant for simulating metallic fluids. However, by using a superposition of two Yukawa-type potentials, we have been able to obtain data for radial distribution function and transport properties, which are in agreement with data derived from a more elaborated potential and from experimental data as well. The softness and attractive part of the potential play a relevant role for obtaining good results for transport properties. For instance, the diffusion is increased for soft particles and an opposite situation is draw for particles with considerable hardness [37]. The attractive interaction also affects the diffusion, when the attraction is increased then the mobility of the particle diminishes. In this work we can modulate the depth and the width of the attractive part of the interaction potential, and at the same time, we are able to modify the softness of the particles with these same parameters. Likewise it is convenient to handle efficiently the long range interactions in a simulation, this point could be more evident estimating the coexistence densities in the liquid–vapor equilibrium.

5. Concluding remarks

The radial distribution function for each metallic fluid obtained by MD shows a good agreement when it was compared with data obtained from different potentials. The β and α parameters for each fluid were fitted, then the transport properties were estimated using the Green–Kubo formula. The transport properties such as self-diffusion and shear viscosity were calculated and compared with the experimental data, and as a result a good agreement was found. By modifying the softness of the particles and the reach of attractive part of the potential, we have obtained results to transport properties and they are quite close to experimental data. This is important for us since we have used a short cut-off radius in all our MD runs and this election on cut-off distance allows us to save computer time.

Finally, we can mention that all our results indicate that the potential works very well on the region near the melting point. In the near future we shall calculate thermodynamic properties at liquid–vapor interface such as surface tension and vapor pressure for these same alkali metals.

Acknowledgements

The authors acknowledge CONACyT-México for partial support, Grands F/52803 and P/49607. JLL thanks to UAEM-México for partial support, Grands 2152/2005 and 2263/2006.

References

[1] S. Sinha, P.L. Srivatava, R.N. Singh. Temperature-dependent structure and electrical transport in liquid metals. *J. Phys.: Condens. Matter*, **1**, 1695 (1989).
[2] M. Silbert, I.H. Umar, M. Watabe, W.H. Young. Young. Entropies and structure factors of liquid metals. *J. Phys. F: Metals Phys.*, **5**, 1262 (1975).
[3] B.P. Alblas, W. van der Lugt. Samll-angle X-ray scattering from sodium-potassium alloys. *J. Phys. F: Metals Phys.*, **10**, 531 (1980).
[4] F.C. Frank. Supercooling of liquids. *Proc. R. Soc. Lond. A*, **215**, 43 (1952).
[5] M. Hasegawa, K. Hoshino, M. Watabe. A theory of melting in metallic small particles. *J. Phys. F: Metals Phys.*, **10**, 619 (1980).
[6] A. Posada-Amarillas, I.L. Garzón. Vibrational analysis of Ni_n clusters. *Phys. Rev. B*, **54**, 10362 (1996).
[7] U. Balucani, A. Torcini, R. Vallauri. Microscopic dynamics in liquid alkali metals. *Phys. Rev. A*, **46**, 2159 (1992).
[8] U. Balucani, A. Torcini, R. Vallauri. Liquid-alkali metals at the melting point: structural and dynamical properties. *Phys. Rev. B*, **47**, 3011 (1993).
[9] R. Evans, T.J. Sluckin. The long-wavelength behaviour of the structure factor of liquid alkali metals. *J. Phys. C: Solid State Phys.*, **14**, 3137 (1981).
[10] M. Tanaka. Molecular dynamics simulation of the structure of liquid rubidium along the saturated vapour-pressure curve. *J. Phys. F: Metal Phys.*, **10**, 2581 (1980).
[11] M.S. Daw, M.I. Baskes. Embedded-atom method: Derivation and application to impurities, surfaces, and other defects in metals. *Phys. Rev. B*, **29**, 6443 (1984).
[12] S.M. Foiles. Application of the embedded-atom method to liquid transition metals. *Phys. Rev. B*, **32**, 3409 (1985).
[13] C. Desgranges, J. Delhommelle. Molecular insight into the pathway to crystallization of aluminum. *J. Am. Chem. Soc.*, **129**, 7012 (2007).
[14] A.W. Jasper, N.E. Schultz, D.G. Truhlar. Analytic potential energy functions for simulating aluminum nanoparticles. *J. Phys. Chem. B*, **109**, 3915 (2005).
[15] D. Bhatt, A.W. Jasper, N.E. Schultz, J.I. Siepmann, D.G. Truhlar. Critical properties of aluminum. *J. Am. Chem. Soc.*, **128**, 4224 (2006).
[16] D. Bhatt, N.E. Schultz, A.W. Jasper, J.I. Siepmann, D.G. Truhlar. Phase behavior of elemental aluminum using Monte Carlo simulations. *J. Phys. Chem. B*, **110**, 26135 (2006).
[17] R.P. Gupta. Lattice relaxation at a metal surface. *Phys. Rev. B*, **23**, 6265 (1981).
[18] M. Matsuda, H. Mori, K. Hoshino, M. Watabe. Universality in the structural change of expanded liquid alkali metals along the liquid-vapour coexistence curve. *J. Phys.: Condens. Matter*, **3**, 827 (1991).

[19] M. Hasegawa, K. Horishino, M. Watabe, W.H. Young. A new simple pseudopotential with applications to liquid metal structure factor calculations. *J. Non-Cryst. Solids*, **117/118**, 300 (1990).
[20] J.A. Anta, P. Madden. Structure and dynamics of liquid lithium: comparison of *ab initio* molecular dynamics predictions with scattering experiments. *J. Phys.: Condens. Matter*, **11**, 6099 (1999).
[21] A. Kietzmann, R. Redmer, F. Hensel, M.P. Desjarlais, T.R. Mattsson. Structure of expanded fluid Rb and Cs: a quantum molecular dynamics study. *J. Phys.: Condens. Matter*, **18**, 5597 (2006).
[22] R.T. Arlinghaus, P.T. Cummings. The role of the pair potential in determining the structure factor of liquid rubidium. *J. Phys. F: Metals Phys.*, **17**, 797 (1987).
[23] D.L. Price, K.S. Singwi, M.P. Tosi. Lattice dynamics of alkali metals in the self-consistent screening theory. *Phys. Rev. B*, **2**, 2983 (1970).
[24] P.M. Morse, E.C.G. Stueckelberg. Diatomic molecules according to the wave mechanics I: Electronic levels of the hydrogen molecular Ion. *Phys. Rev.*, **33**, 932 (1929).
[25] M.P. Allen, D.J. Tildesley. *Computer Simulation of Liquids*, pp. 50–64, pp. 146–149, Clarendon Press, Oxford 146–149 (2003).
[26] D. Osorio-Gonźalez, M. Mayorga, J. Orozco, L. Romero-Salazar. Entropy and thermalization of particles in liquids. *J. Chem. Phys.*, **118**, 6989 (2003).
[27] U.F. Galicia-Pimentel, D. Osorio-Gonźalez, J. López-Lemus. On the Morse potential in liquid phase and at liquid-vapor interface. *Rev. Mex. Fis.*, **52**, 422 In English (2006).
[28] J.K. Singh, J. Adhikari, S.K. Kwak. Vapor-liquid phase coexistence curves for Morse fluids. *Fluid Phase Equilib.*, **248**, 1 (2006).
[29] J.P.K. Doye, D.J. Wales. The structure and stability of atomic liquids: from clusters to bulk. *Science*, **271**, 484 (1996).
[30] X. Xu, C. Cheng, I.H. Chowdhury. Molecular dynamics study of phase change mechanisms during femtosecond laser ablation. *J. Heat Transfer*, **126**, 727 (2004).
[31] D. Ruelle. *Statistical Mechanics: Rigorous Results*, pp. 29–41, World Scientific/Imperial College Press, London (1999).
[32] S. Nosé. A molecular dynamics for simulations in the canonical ensemble. *Mol. Phys.*, **52**, 255 (1984); W.G. Hoover, Canonical dynamics: equilibrium phase-space distributions. *Phys. Rev. A*, **31**, 1985, 1695 (1984).
[33] S. Melchionna, G. Ciccotti, B.L. Holian. Hoover NPT dynamics for systems varying in shape and size. *Mol. Phys.*, **78**, 533 (1993).
[34] Chem-Globe database, Latent heat of fusion for alkali metals. The numerical values were taken from Chem-Globe database. Available online at: http://-pol.spurious.biz/projects/chemglobe/ptoe, accessed 10 June 2007 (2007).
[35] E. Urrutia-Bañuelos, A. Posadas-Amarillas. Efecto de la temperatura en las propiedades estructurales y dinámicas de Ag líquida: un estudio con dinámica molecular. *Rev. Mex. Fís.*, **50**, 53 (2004).
[36] J. López-Lemus, J. Alejandre. Thermodynamic and transport properties of simple fluids using lattice sums: bulk phases and liquid-vapour interface. *Mol. Phys.*, **100**, 2983 (2002).
[37] M. Canales, J.A. Padró. Dynamics properties of Lennard-Jones fluids and liquid metals. *Phys. Rev. E*, **60**, 551 (1999).